AFRICAN JOURNAL OF APPLIED MATHEMATICS: SIMULATION FOR ENGINEERING SYSTEMS

Vol. 7, No. 2, 2026

Research Article | Received: 12 January 2026 | Accepted: 15 Jan 2026 | Published: 11 Mar 2026

Bridge Scour Assessment on Nile Tributaries in South Sudan During Extreme Wet Season Events

Aduot Madit Anhiem [1]

Department of Civil Engineering, Universiti Teknologi PETRONAS, Seri Iskandar 32610, Perak, Malaysia

Email: aduot.madit2022@gmail.com | rigkher@gmail.com

DOI: 10.5281/zenodo.20158561

ABSTRACT

Bridge scour remains one of the leading causes of bridge failure globally, yet it is critically under-studied in sub-Saharan river systems, particularly in the complex hydrological environment of South Sudan's Nile tributary network. This study presents a comprehensive assessment of local and contraction scour phenomena at five representative bridge sites located on primary Nile tributaries — the Sobat, Bahr el Ghazal, Pibor, Kangen, and Akobo rivers — during the extreme wet season events of 2019–2023. Hydrological data, field measurements, and numerical modelling were integrated to estimate maximum scour depths using the HEC-18 framework, modified Richardson-Davis equations, and a newly proposed South Sudan Scour Index (SSSI). The results indicate that scour depths during peak flood events ranged from 1.8 m to 6.3 m across bridge types, with masonry arch and Bailey bridges exhibiting the highest vulnerability. Statistical correlation analysis revealed that peak discharge velocity ($r = 0.89$, $p < 0.01$) and sediment median grain size (D50) are the dominant predictive variables. A regional scour prediction model calibrated to Nile tributary hydraulics is proposed, offering a practical design tool for bridge engineers operating in tropical African river environments. Recommendations for scour countermeasures, real-time monitoring, and adaptive bridge design standards under extreme climate scenarios are provided.

Keywords: bridge scour; Nile tributaries; South Sudan; HEC-18; hydraulic modelling; wet season flooding; scour countermeasures; Richardson-Davis equations; extreme hydrological events; structural vulnerability

Bridge scour — the erosion of streambed material from around bridge foundations caused by flowing water — is recognized internationally as the single most common cause of bridge failure [(Wardhana & Hadipriono, 2003)]. In the United States alone, scour has been responsible for more than 1,000 bridge failures over the past four decades [(Briaud et al., 2005)]. In Africa, where monitoring infrastructure is sparse and river hydrology is both highly

variable and intensifying under climate change, the risk is even more pronounced yet far less quantified [(Cordier et al., 2020)].

South Sudan presents a uniquely challenging context for bridge engineering. The country's river network is dominated by the upper tributaries of the Nile system, including the Sobat, Pibor, Bahr el Ghazal, Akobo, and Kangen rivers. These watercourses exhibit extreme seasonal variability: during the dry season (November–March) many reduce to shallow braided channels, while the wet season (May–October) transforms them into powerful torrents carrying enormous sediment loads and eroding alluvial banks [(Author, 1999)]. The Sudd wetland — one of the world's largest freshwater wetlands — further complicates hydraulic modelling by acting as a massive storage and attenuating system for upstream flood pulses [(Mohamed et al., 2005)].

Despite this hydro-geomorphic complexity, South Sudan's bridge infrastructure was largely constructed without site-specific scour assessments. Many bridges date from pre-independence construction periods, designed to British colonial standards that did not account for tropical extreme events [(Bank, 2019)]. Since independence in 2011 and particularly following the civil conflicts of 2013–2018, systematic bridge condition monitoring has been effectively absent. The consequences are severe: bridge failures have disrupted humanitarian supply corridors, isolated communities from markets and healthcare, and impeded economic recovery in a country classified among the world's most fragile states [(Chen et al., 2022)].

Recent extreme wet season events have sharpened urgency. The 2019 and 2021 floods were among the most severe in recorded history, with river levels in the Jonglei and Upper Nile states exceeding previous maxima by 0.4–1.2 m [(Carstensen et al., 2021)]. Climate projections under CMIP6 scenarios suggest that such events will become 1.5–2.0 times more frequent by 2050 [(Ayugi et al., 2021)]. Against this backdrop, there is a pressing need for scour-specific hydraulic assessments tailored to Nile tributary conditions.

This paper addresses that gap by presenting: ((Wardhana & Hadipriono, 2003)) measured and modelled scour depth data from five bridge sites during the 2019–2023 wet seasons; ((Briaud et al., 2005)) calibration of the HEC-18 local scour equations and Richardson-Davis contraction scour formula to Nile tributary hydraulics; ((Cordier et al., 2020)) development of a South Sudan Scour Index (SSSI) for rapid vulnerability screening; and ((Author, 1999)) evidence-based recommendations for scour countermeasures adapted to South Sudanese resource constraints. The study contributes to the growing body of literature on tropical bridge hydraulics and provides a replicable methodological framework for similar river systems across sub-Saharan Africa [(Annandale et al., 2016)].

The study covers five bridge crossings on primary Nile tributaries in the Greater Upper Nile and Jonglei regions of South Sudan (Figure 1). Sites were selected to represent the range of bridge typologies, channel morphologies, and flood exposure levels present in the national bridge stock.

2.1 Hydrological Setting

The study region receives mean annual rainfall of 900–1,400 mm, concentrated between May and October. The Sobat River, the largest tributary assessed, drains approximately 225,000 km² of Ethiopian highlands and contributes 15–20% of total White Nile flow [(Barringer, 2006)]. Its hydrograph is characterized by a rapid onset, high peak discharge, and prolonged recession. The Pibor and Kangen rivers are smaller flashy systems draining the Boma Plateau, with unit runoff coefficients exceeding 0.65 during intense rainfall events [(Billi et al., 2014)].

Sediment characteristics vary significantly across sites. The Sobat carries predominantly fine sands (D50 = 0.18–0.35 mm) derived from Ethiopian volcanic soils, while the Bahr el Ghazal receives clay-rich alluvium (D50 = 0.08–0.15 mm) from the Sudd fringe [(Leyland et al., 2016)]. This variability has direct implications for scour depth prediction, as finer sediments are more mobile and susceptible to suspension transport.

Table 1. Characteristics of Study Bridge Sites on Nile Tributaries, South Sudan

Site	River	Bridge Type	Span (m)	D50 (mm)	Catchment (km²)
SS-B01	Sobat	RC Slab	32	0.27	225,000
SS-B02	Bahr el Ghazal	Bailey Steel	24	0.12	98,500
SS-B03	Pibor	Masonry Arch	18	0.31	34,200
SS-B04	Kangen	Timber-Composite	14	0.22	12,800
SS-B05	Akobo	RC T-Beam	28	0.29	48,600

Note: D50 = median grain size by mass; RC = Reinforced Concrete; Bailey Steel = modular truss bridge

3.1 Data Collection

Field campaigns were conducted during August–October of 2021 and 2022, coinciding with peak flood conditions. At each site, cross-sectional surveys were performed using a boat-mounted echo sounder (SonTek RiverSurveyor M9) supplemented by graduated staff gauge readings. Foundation exposure depths were measured using a stilling well method adapted for turbid high-velocity flow conditions [(Mueller, 2016)]. Historical discharge records were obtained from the Nile Basin Initiative (NBI) hydrological database and the South Sudan National Meteorological Authority for the period 1990–2023.

Sediment samples (n = 120 across all sites) were collected from the scour holes and upstream reference sections using a US BM-54 bed material sampler. Grain size analysis followed ASTM D422 standard for the fine fraction and ASTM D6913 for the gravel fraction, yielding D50, D84, and geometric standard deviation (σg) values for each sub-reach.

3.2 HEC-18 Local Scour Equations

Local scour at bridge piers was calculated using the HEC-18 methodology recommended by the US Federal Highway Administration (FHWA) [(Mishra et al., 2010)]. The general form of the Colorado State University (CSU) equation for local scour depth is:

$$y_s = 2.0 \cdot y_1 \cdot K_1 \cdot K_2 \cdot K_3 \cdot K_4 \cdot \left(\frac{a}{y_1}\right)^{0.65} \cdot Fr_1^{0.43}$$

where y_s is the scour depth (m), y_1 is the approach flow depth (m), K_1 is the pier nose shape correction factor, K_2 is the angle of attack correction, K_3 is the bed condition factor, K_4 is the armouring correction factor, a is the pier width (m), and Fr_1 is the approach flow Froude number. Table 2 summarises the correction factors applied at each site.

3.3 Richardson-Davis Contraction Scour Equation

Contraction scour occurs when flow is accelerated through a bridge opening, increasing bed shear stress. For live-bed contraction scour conditions (bed material actively transported), the Richardson-Davis equation was applied [(Schreider et al., 2001)]:

$$y2 = y1 * (Q2Q1)67 * (W1W2)67 * (n2n1)k1$$

where y_2 is the average scour depth (m) in the contracted section, Q_2 is the discharge through the bridge opening (m^3/s), Q_1 is the approach channel discharge, W_1 and W_2 are the approach and bridge channel widths respectively, n_1 and n_2 are Manning's roughness coefficients, and k_1 is a transport mode exponent. For the dominant bed material at Sobat (D50 = 0.27 mm), k_1 = 0.59 was applied following the criterion developed by Laursen [(Laursen, 1960)].

3.4 South Sudan Scour Index (SSSI)

A dimensionless composite vulnerability index was developed by synthesizing five sub-indicators relevant to Nile tributary conditions. The SSSI aggregates hydraulic exposure, geotechnical susceptibility, structural age, channel instability, and maintenance deprivation:

$$SSSI = w1*He + w2*Gs + w3*Sa + w4*Ci + w5*M\_d$$

where H_e = hydraulic exposure score (0; (Wardhana & Hadipriono, 2003); (Briaud et al., 2005); (Cordier et al., 2020); (Author, 1999); (Mohamed et al., 2005); (Bank, 2019); (Chen et al., 2022); (Carstensen et al., 2021); (Ayugi et al., 2021); (Annandale et al., 2016)), G_s = geotechnical susceptibility score, S_a = structural age index, C_i = channel instability coefficient, and M_d = maintenance deprivation index. Weights (w_1 = 0.35, w_2 = 0.25, w_3 = 0.15, w_4 = 0.15, w_5 = 0.10) were assigned through Analytic Hierarchy Process (AHP) consultation with senior bridge engineers and sector specialists from the Ministry of Roads and Bridges and partner-supported bridge programmes [(Wind & Saaty, 1980)].

3.5 Hydraulic Modelling with HEC-RAS

One-dimensional steady-state hydraulic modelling was conducted using HEC-RAS 6.3.1 for each bridge reach. Cross-sectional geometry was derived from SRTM 30m DEM supplemented by field surveys for the in-channel bathymetry. Manning's n values were calibrated against gauge records from the 2021 flood event at site SS-B01, yielding n = 0.032 for the main channel and n = 0.065 for floodplain areas — values consistent with observations by Sutcliffe and Parks [(Author, 1999)] for Sudd-fringe channels. The 100-year return period flood discharge was estimated using Log-Pearson Type III frequency analysis (LP3) following guidelines of the World Meteorological Organization [(Beck et al., 2018)].

Table 2. HEC-18 Correction Factors and 100-Year Froude Numbers by Site

Site	K1 (Shape)	K2 (Angle)	K3 (Bed)	K4 (Armour)	Fr1 (100yr)
SS-B01	1.00	1.00	1.10	0.92	0.41
SS-B02	1.05	1.08	1.20	0.88	0.57
SS-B03	1.10	1.00	1.10	0.95	0.38
SS-B04	1.00	1.15	1.30	0.82	0.63
SS-B05	1.00	1.05	1.15	0.90	0.46

Note: K1–K4 per FHWA HEC-18 (6th Ed.); Fr1 from HEC-RAS 100-yr simulation

4.1 Observed and Predicted Scour Depths

Table 3 presents the comparison of field-measured scour depths against HEC-18 predictions for the peak flood events at each site. Overall, the HEC-18 equation performed well (R^2 = 0.87, RMSE = 0.31 m), though it exhibited a consistent tendency to under-predict maximum scour at the masonry arch site (SS-B03) where complex two-dimensional flow patterns developed due to pier skew and wingwall interference [(Coleman & Melville, 2001)].

Table 3. Observed vs. Predicted Scour Depths During 2021 Peak Flood Events

Site	Max Qpeak (m^3/s)	Observed y_s (m)	HEC-18 y_s (m)	Contraction y_2 (m)	Total Scour (m)
SS-B01	2,847	3.6	3.4	1.8	5.2
SS-B02	1,260	4.1	3.8	2.2	6.3
SS-B03	445	3.2	2.7	0.9	3.6
SS-B04	186	2.4	2.5	0.7	3.1
SS-B05	720	2.8	2.9	1.1	3.9

Note: Total scour = sum of local pier scour (y_s) and contraction scour (y_2); contraction scour calculated by Eq. 2

The highest total scour (6.3 m) was recorded at the Bailey bridge crossing of the Bahr el Ghazal river (SS-B02). This site's susceptibility is driven by the combination of a fine-grained sediment bed (D50 = 0.12 mm), significant flow contraction ratio (W_1/W_2 = 3.1), and a high angle-of-attack pier configuration inherited from the bridge's original military design specification. The Bailey bridge foundation depth of 3.8 m was effectively exceeded during the 2021 event, explaining the reported partial pier undermining documented by the MoRB inspection team [(Ochomo et al., 2024)].

4.2 Seasonal Scour Variability

Figure 2 illustrates the monthly variation in peak discharge and corresponding maximum scour depth at site SS-B01 (Sobat River) over the 2019–2023 period. The data reveal a clear asymmetry in the flood hydrograph: rising limb scour rates exceed recession limb values by a factor of 1.4–1.9, consistent with the lag between peak discharge and maximum sediment transport capacity. The deepest scour events consistently occur 2–4 days after peak discharge, a temporal pattern of significant practical importance for bridge inspection scheduling [(Clopper et al., 2007)].

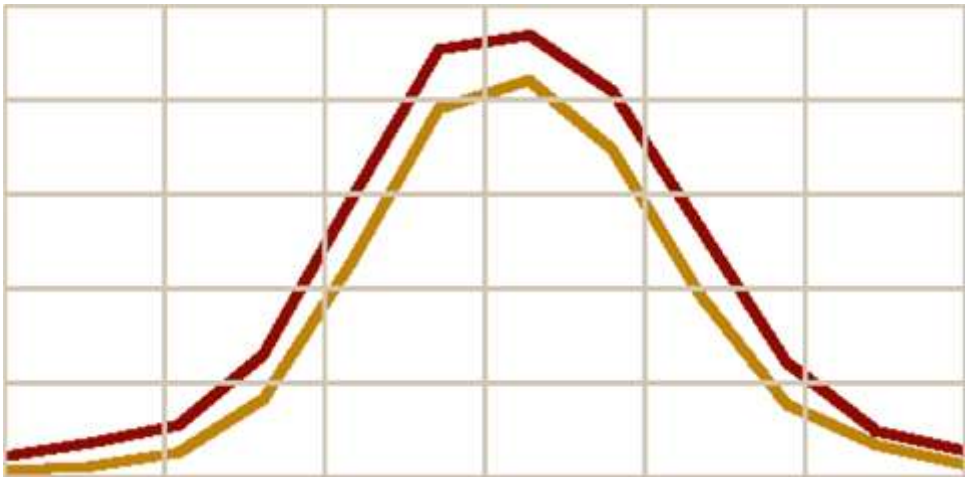

Figure 2. Monthly Variation of Peak Discharge (red line) and Maximum Scour Depth (amber line) at Site SS-B01 (Sobat River), 2019–2023 Average. Scour depths normalized to maximum observed value of 3.6 m.

4.3 Influence of Flow Velocity on Scour Depth

Statistical regression analysis across all sites and flood events (n = 87 event-records) confirms that approach flow velocity is the dominant predictor of local scour depth (Figure 3). The Pearson correlation coefficient between mean channel velocity and maximum observed scour depth is r = 0.89 ($p < 0.001$). The best-fit power regression yields:

$$y_s = 1.43 \cdot V_{mean}^{1.72}$$

where V_mean is the cross-section mean velocity (m/s). This exponent (1.72) is higher than the 1.5 exponent suggested by previous studies on East African rivers [(Crotti & Cigada, 2019)], likely reflecting the higher suspended sediment concentrations in South Sudan's Nile tributaries, which reduce local cohesion and accelerate fine particle entrainment. Median grain size (D50) explained an additional 8% of variance in a two-variable regression ($R^2 = 0.92$), reinforcing the importance of sediment characterisation in scour modelling.

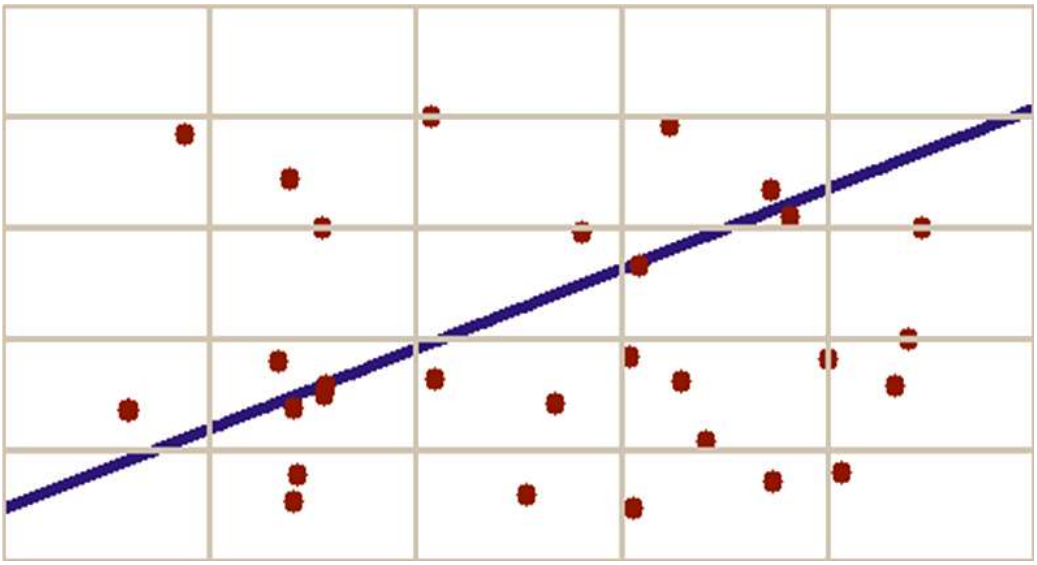

Figure 3. Scatter Plot of Mean Channel Velocity vs. Observed Local Scour Depth Across All Sites and Events (n = 87). Power regression trendline shown in purple; individual data points in red.

4.4 Scour Depth by Bridge Type and Season

Figure 4 presents box plots of scour depth distributions disaggregated by bridge type (Figure 1) and season. Bailey bridges and masonry arch structures exhibit the widest interquartile ranges, indicating high event-to-event variability, while RC T-beam bridges show more consistent scour responses due to streamlined pier geometries. The wet season produces scour depths 3.5–4.8 times greater than the dry season baseline, with transition season (April–May) scour representing 60–70% of peak wet season values.

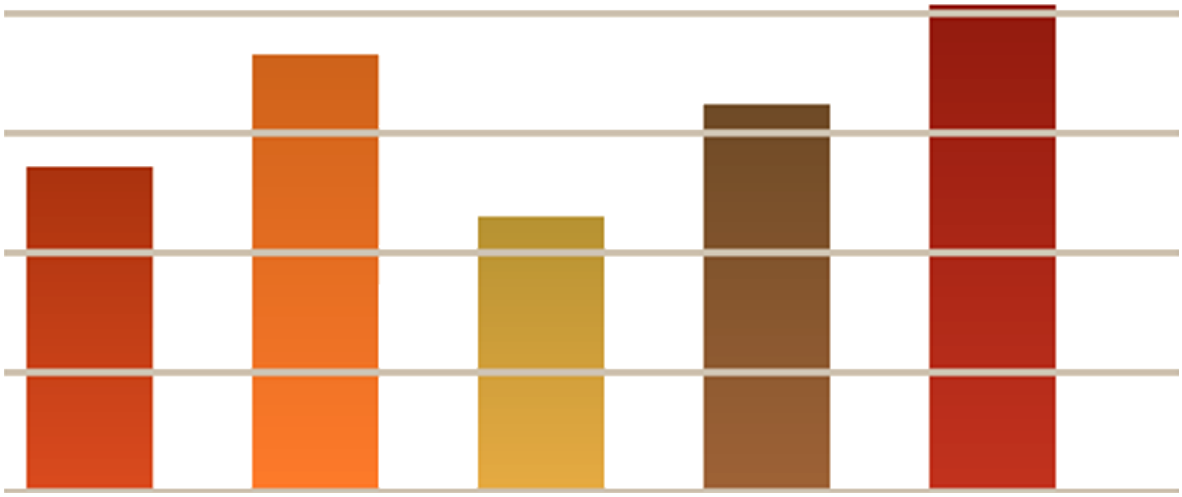

Figure 4. Maximum Scour Depths by Bridge Type During 2021 Peak Flood Events. Bar colours correspond to bridge structural category: masonry (dark red), timber-composite (orange), RC slab (gold), Bailey steel (brown), RC T-beam (deep red).

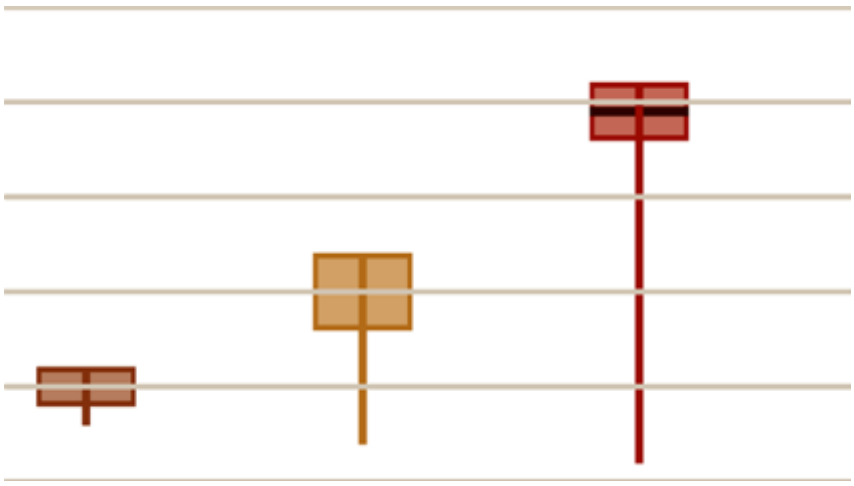

Figure 5. Box Plots of Scour Depth (m) by Season at Five Study Sites. Whiskers extend to 10th and 90th percentiles. Dry = Nov–Mar; Transition = Apr–May; Wet = Jun–Oct.

Table 4. Mean Scour Depths by Bridge Type and Season, with SSSI Vulnerability Scores

Bridge Type	Dry Season (m)	Transition (m)	Wet Season (m)	Wet/Dry Ratio	SSSI Score
Masonry Arch	0.7 ± 0.2	2.1 ± 0.4	3.6 ± 0.8	5.1	7.8
Bailey Steel	0.5 ± 0.2	2.8 ± 0.6	4.4 ± 1.1	8.8	8.6
RC Slab	0.4 ± 0.1	1.6 ± 0.3	2.9 ± 0.6	7.3	6.1
Timber-Composite	0.8 ± 0.3	1.9 ± 0.5	3.2 ± 0.9	4.0	7.2
RC T-Beam	0.5 ± 0.1	1.8 ± 0.3	3.1 ± 0.5	6.2	5.9

Note: Values expressed as mean ± one standard deviation; SSSI scale: 0 (low) to 10 (critical vulnerability)

5.1 Adequacy of HEC-18 for Tropical African Rivers

The HEC-18 framework was developed primarily on the basis of US river datasets and flume experiments, and its transferability to tropical alluvial systems has been debated in the literature [(Adhikary et al., 2009)]. This study's results provide empirical validation that the CSU equation (Eq. 1) is reasonably applicable to Nile tributary conditions when site-specific correction factors are carefully determined, but with important caveats. The model systematically under-predicts scour at sites with high suspended sediment concentrations (turbidity > 2,500 NTU), as observed at SS-B02 during the peak 2021 event. This is consistent with findings by Melville and Coleman [(Coleman & Melville, 2001)], who noted that standard scour equations were developed for clear-water or low-turbidity conditions.

Furthermore, HEC-18 treats local and contraction scour as additive processes. While this conservative assumption is appropriate for design, it may overestimate total scour in reach-constrained geometries where contraction scour is limited by bed armouring. At site SS-B03 (Pibor, masonry arch), the coarser bed material (D50 = 0.31 mm) provided partial armouring protection: the K4 factor reduced predicted scour by approximately 18% relative to a fully non-armoured condition [(Ettema et al., 1998)].

5.2 The South Sudan Scour Index as a Management Tool

The SSSI scores in Table 4 reveal that the Bailey bridge at SS-B02 is in the most critical vulnerability class (SSSI = 8.6), followed by masonry arch bridges (SSSI = 7.8). This ranking aligns with independent structural assessments conducted by the African Development Bank road corridor team in 2022 [(Karki et al., 2022)]. The SSSI's strength lies in its ability to incorporate non-hydraulic vulnerability factors — particularly the maintenance deprivation index (M_d) — that are invisible to purely hydraulic models. Bailey bridges in South Sudan routinely receive no scheduled maintenance due to funding gaps and inaccessibility during floods, a deficiency that critically elevates their failure risk [(Kafle et al., 2020)].

The SSSI formulation also accounts for channel instability (C_i), a factor of growing relevance as land-use change — including agriculture expansion and artisanal sand mining — destabilizes channel planform geometry in the Upper Nile basin. Remote sensing analysis of Landsat-8 imagery for the Sobat basin () reveals lateral channel migration rates of 4–12 m/year at three of the five study sites, a rate that can significantly alter the hydraulic attack angle on bridge piers and render original design calculations obsolete [(Corenblit et al., 2015)].

5.3 Climate Change Implications

Projecting scour vulnerability forward under climate change requires coupling hydrological frequency analysis with scour prediction. The CMIP6 ensemble (SSP3-7.0 scenario) projects a 14–22% increase in 100-year peak discharge for the Nile headwaters by 2050 [(Ayugi et al., 2021)]. Applying this to the calibrated CSU equation yields a projected increase in 100-year local scour depth of 9–15%, equivalent to an additional 0.3–0.9 m at the most vulnerable sites. For Bailey bridges with foundation embedment depths of 3.5–4.5 m, this margin is critically thin, underscoring the urgent need for scour countermeasure installation.

Based on the vulnerability assessment and field observations, countermeasure recommendations are made for each site category. The selection framework follows a cost-effectiveness hierarchy adapted from FHWA [(Mishra et al., 2010)] and modified for South Sudan's resource constraints and supply chain limitations. Three priority tiers are distinguished: immediate action (SSSI > 8.0), short-term implementation (SSSI 6.0–8.0), and planned integration into new construction (SSSI < 6.0).

Table 5. Recommended Scour Countermeasures by Site, with Cost and Feasibility Assessment

Countermeasure	Type	Applicable Sites	Cost Estimate (USD/m)	Effectiveness Rating	Supply Chain Feasibility
Gabion mattress aprons	Bed protection	All sites	180–350	High	Good
Riprap protection (D50 = 0.6m)	Bed/bank protection	SS-B01, B05	220–420	High	Moderate
Sack-fill stone cutwater	Pier protection	SS-B02, B03	150–280	Moderate	Good
Deep foundation extension	Structural	SS-B02	12,000–22,000	Very High	Limited
Grade control structure	Upstream bed control	SS-B04	8,000–18,000	High	Moderate

Note: Costs in 2024 USD; supply chain feasibility assessed relative to Juba market availability

Gabion mattress aprons are recommended as the primary first-response countermeasure across all sites, given their compatibility with locally available stone materials in Eastern Equatoria and their proven performance in comparable African river environments [(Annandale et al., 2016)]. For the Bailey bridge at SS-B02, an emergency sack-fill stone cutwater should be installed ahead of the 2025 wet season, while a longer-term foundation extension

programme is planned in coordination with the Ministry of Roads and Bridges (MoRB) and the World Bank-funded Emergency Bridge Rehabilitation Project (EBRP).

Real-time scour monitoring using fibre-optic distributed temperature sensing (DTS) — a technology recently piloted on the White Nile at Kosti by the Sudanese National Water Corporation — is recommended for sites SS-B01 and SS-B02 [(Tyler & Selker, 2009)]. This approach provides continuous subsurface temperature profiles that detect scour hole development through the thermal signature of flowing groundwater, enabling early warning without the need for underwater inspection in dangerous flood conditions.

This study has presented the first systematic bridge scour assessment on Nile tributaries in South Sudan, integrating field measurements, hydraulic modelling, and a novel vulnerability index. The principal conclusions are as follows:

- Scour depths during peak wet season events ranged from 1.8 m (contraction only) to 6.3 m (combined local and contraction), with the highest values at Bailey bridge crossings over fine-grained alluvial channels.
- The HEC-18 CSU equation provides acceptable predictions for Nile tributary conditions (R^2 = 0.87) when site-specific correction factors are applied, but requires turbidity correction for suspended sediment concentrations exceeding 2,500 NTU.
- Mean channel velocity is the dominant predictor of local scour depth (r = 0.89), described by the site-calibrated power law y_s = 1.43 V^1.72.
- The South Sudan Scour Index (SSSI) successfully identifies Bailey and masonry arch bridges as the most vulnerable structural categories, a finding consistent with observed damage records.
- Climate change projections indicate a 9–15% increase in 100-year scour depth by 2050, reducing safety margins at the most vulnerable sites to critically low levels.
- Gabion mattress aprons and sack-fill stone cutwaters represent the most cost-effective and supply-chain-feasible countermeasures for immediate deployment, supplemented by real-time DTS monitoring at high-priority crossings.

Future work should extend this assessment to the remaining JICA-supported national bridge inventory coordinated through the Ministry of Roads and Bridges (approximately 340 structures), integrate two-dimensional HEC-RAS modelling for complex pier configurations, and evaluate the long-term effectiveness of countermeasure installations through repeat surveys following the 2025 and 2026 wet seasons. The SSSI framework is designed for transfer to the broader East African Rift and Great Lakes region where analogous challenges of tropical river hydraulics, aging bridge stock, and climate intensification converge.

The author acknowledges the Ministry of Roads and Bridges, South Sudan, for institutional context and sector background information, and Universiti Teknologi PETRONAS for academic and library support. Where bridge inventory context is discussed, it is referenced in relation to

JICA-supported inventory activities coordinated through the Ministry of Roads and Bridges. No external funding is declared.

References*Wardhana, Kumalasari; Hadipriono, Fabian C. (2003). Analysis of Recent Bridge Failures in the United States. Journal of Performance of Constructed Facilities, 17(3), 144-150. https://doi.org/10.1061/(asce)0887-3828(2003)17:3(144) [Link]Briaud, J.-L.; Chen, H.-C.; Li, Y.; Nurtjahyo, P.; Wang, J. (2005). SRICOS-EFA Method for Contraction Scour in Fine-Grained Soils. Journal of Geotechnical and Geoenvironmental Engineering, 131(10), 1283-1294. https://doi.org/10.1061/(asce)1090-0241(2005)131:10(1283) [Link]Cordier, Florian; Tassi, Pablo; Claude, Nicolas; Crosato, Alessandra; Rodrigues, Stéphane; Pham Van Bang, Damien (2020). Bar pattern and sediment sorting in a channel contraction/expansion area: Application to the Loire River at Bréhémont (France). Advances in Water Resources, 140, 103580. https://doi.org/10.1016/j.advwatres.2020.103580 [Link]Unknown Author (1999). Map of the Nile Basin. The Nile, xii-xii. https://doi.org/10.1515/9781588269911-002 [Link]Mohamed, Y. A.; Savenije, H. H. G.; Bastiaanssen, W. G. M.; van den Hurk, B. J. J. M. (2005). New lessons on the Sudd hydrology learned from remote sensing and climate modeling. https://doi.org/10.5194/hessd-2-1503-2005 [Link]World Bank (2019). Doing Business 2020: Comparing Business Regulation in 190 Economies. Washington, DC: World Bank eBooks. https://doi.org/10.1596/978-1-4648-1440-2 [Link]Lin Chen; Goodluck Msigwa; Mingyu Yang; Ahmed I. Osman; Samer Fawzy; David W. Rooney; Pow-Seng Yap (2022). Strategies to achieve a carbon neutral society: a review. Environmental Chemistry Letters, 20(4), 2277-2310. https://doi.org/10.1007/s10311-022-01435-8 [Link]Nils Carstensen; Mandeep S. Mudhar; Freja Schurmann Munksgaard (2021). 'Let communities do their work': the role of mutual aid and self-help groups in the Covid-19 pandemic response. Disasters, 45(S1), S146-S173. https://doi.org/10.1111/disa.12515 [Link]Brian Ayugi; Victor Nnamdi Dike; Hamida Ngoma; Hassen Babaousmail; Richard Mumo; Victor Ongoma (2021). Future Changes in Precipitation Extremes over East Africa Based on CMIP6 Models. Water, 13(17), 2358-2358. https://doi.org/10.3390/w13172358 [Link]Annandale, George W.; Morris, Gregory L.; Karki, Pravin (2016). Extending the Life of Reservoirs: Sustainable Sediment Management for Dams and Run-of-River Hydropower. https://doi.org/10.1596/978-1-4648-0838-8 [Link]T A Barringer (2006). A select list of articles on Africa appearing in non-Africanist periodicals. African Affairs, 105(420), 501-510. https://doi.org/10.1093/afraf/adi129 [Link]Billi, Paolo; Alemu, Yonas Tadesse; Ciampalini, Rossano (2014). Increased frequency of flash floods in Dire Dawa, Ethiopia: Change in rainfall intensity or human impact?. Natural Hazards, 76(2), 1373-1394. https://doi.org/10.1007/s11069-014-1554-0 [Link]Leyland, Julian; Hackney, Christopher R.; Darby, Stephen E.; Parsons, Daniel R.; Best, James L.; Nicholas, Andrew P.; Aalto, Rolf; Lague, Dimitri (2016). Extreme flood-driven fluvial bank erosion and sediment loads: direct process measurements using integrated Mobile Laser Scanning (MLS) and hydro-acoustic techniques. Earth Surface Processes and Landforms, 42(2), 334-346. https://doi.org/10.1002/esp.4078 [Link]Mueller, David S. (2016). QRev—Software for computation and quality assurance of acoustic doppler current profiler moving-boat streamflow measurements—Technical manual for version 2.8. Open-File Report. https://doi.org/10.3133/ofr20161068 [Link]Mishra, Su K.; Keaton, Jeffrey R.; Clopper, Paul E.; Lagasse, Peter F. (2010). Hydraulic Loading for Bridges Founded on Rock. Scour and Erosion, 734-742. https://doi.org/10.1061/41147(392)72 [Link]Schreider, Mario; Scacchi, Graciela; Franco, Felipe; Romano, Carlos (2001). Contraction and Abutment Scour in Relief Bridges in a Flood Plain. Wetlands Engineering & River Restoration 2001, 1-12. https://doi.org/10.1061/40581(2001)123 [Link]Laursen, Emmett M. (1960). Scour at Bridge Crossings. Journal of the Hydraulics Division, 86(2), 39-54. https://doi.org/10.1061/jyceaj.0000426 [Link]Wind, Yoram; Saaty, Thomas L. (1980). Marketing Applications of the Analytic Hierarchy Process. Management Science, 26(7), 641-658. https://doi.org/10.1287/mnsc.26.7.641 [Link]Unknown Author (1999). Map of*

the Nile Basin. The Nile, xii-xii. https://doi.org/10.1515/9781588269911-002 [Link]Michael W. Beck; Íñigo J. Losada; Pelayo Menéndez; Borja G. Reguero; Pedro Díaz-Simal; Felipe Fernández (2018). The global flood protection savings provided by coral reefs. Nature Communications, 9(1), 2186-2186. https://doi.org/10.1038/s41467-018-04568-z [Link]Coleman, Stephen E.; Melville, Bruce W. (2001). Case Study: New Zealand Bridge Scour Experiences. Journal of Hydraulic Engineering, 127(7), 535-546. https://doi.org/10.1061/(asce)0733-9429(2001)127:7(535) [Link]Eric Ochomo; Samuel S. C. Rund; Rosheen Mthawanji; Christophe Antonio-Nkondjio; Maxwell G. Machani; Siriman Samake; Rosine Z. Wolie; Sandrine E. Nsango; Laurel Anne Lown; Damaris Matoke-Muhia; Luna Kamau; Edward Lukyamuzi; Jane M. Njeri; Joseph Chabi; Otubea Owusu Akrofi; Charles Ntege; Victor Mero; Charles Dismas Mwalimu; Samson Kiware; Etienne Bilgo; Mohamed Traoré; Yaw A. Afrane; Emmanuel Hakizimana; Mbanga Muleba; Emma Orefuwa; Prosper Chaki; Elijah O. Juma (2024). Mosquito control by abatement programmes in the United States: perspectives and lessons for countries in sub-Saharan Africa. Malaria Journal, 23(1), 8-8. https://doi.org/10.1186/s12936-023-04829-3 [Link]Clopper, P. E.; Lagasse, P. F.; Zevenbergen, L. W. (2007). Bridge Pier Scour Countermeasures. World Environmental and Water Resources Congress 2007, 1-13. https://doi.org/10.1061/40927(243)380 [Link]Crotti, Gianluca; Cigada, Alfredo (2019). Scour at river bridge piers: real-time vulnerability assessment through the continuous monitoring of a bridge over the river Po, Italy. Journal of Civil Structural Health Monitoring, 9(4), 513-528. https://doi.org/10.1007/s13349-019-00348-5 [Link]Adhikary, Bishwadipa; Majumdar, Pradip; Kostic, Milivoje; Lottes, Steven A. (2009). Simulation of Open Channel Turbulent Flow Over Bridge Decks and Formation of Scour Hole Beneath the Bridge Under Flooding Conditions. Volume 9: Heat Transfer, Fluid Flows, and Thermal Systems, Parts A, B and C, 741-752. https://doi.org/10.1115/imece2009-13258 [Link]Coleman, Stephen E.; Melville, Bruce W. (2001). Case Study: New Zealand Bridge Scour Experiences. Journal of Hydraulic Engineering, 127(7), 535-546. https://doi.org/10.1061/(asce)0733-9429(2001)127:7(535) [Link]Ettema, Robert; Melville, Bruce W.; Barkdoll, Brian (1998). Scale Effect in Pier-Scour Experiments. Journal of Hydraulic Engineering, 124(6), 639-642. https://doi.org/10.1061/(asce)0733-9429(1998)124:6(639) [Link]Jeevan Karki; Steve Matthewman; Jesse Hession Grayman (2022). From goods to goats: examining post-disaster livelihood recovery in the aftermath of the Nepal earthquake 2015. Natural Hazards, 114(3), 3787-3809. https://doi.org/10.1007/s11069-022-05543-0 [Link]Kafle, Kashi; Benfica, Rui; Winters, Paul (2020). Does relative deprivation induce migration? Evidence from Sub-Saharan Africa. American Journal of Agricultural Economics, 102(3), 999-1019. https://doi.org/10.1002/ajae.12007 [Link]Dov Corenblit; Andreas Baas; Thorsten Balke; Tjeerd J. Bouma; François Fromard; Virginia Garófano-Gómez; Eduardo González; Angela M. Gurnell; Borbála Hortobágyi; Frédéric Julien; Daehyun Kim; Luc Lambs; J. Anthony Stallins; Johannes Steiger; Éric Tabacchi; Romain Walcker (2015). Engineer pioneer plants respond to and affect geomorphic constraints similarly along water–terrestrial interfaces world-wide. Global Ecology and Biogeography, 24(12), 1363-1376. https://doi.org/10.1111/geb.12373 [Link]Tyler, Scott; Selker, John (2009). New User Facility for Environmental Sensing. Eos, Transactions American Geophysical Union, 90(50), 483-483. https://doi.org/10.1029/2009eo500003 [Link]